# A Novel Nine-lncRNA Risk Signature Correlates With Immunotherapy in Hepatocellular Carcinoma

Ye Nie [1,2†], Jianhui Li [1,2†], Wenlong Wu [2†], Dongnan Guo [3], Xinjun Lei [1,2], Tianchen Zhang [1,2], Yanfang Wang [1,2], Zhenzhen Mao [1,2], Xuan Zhang [2] and Wenjie Song [2*]

[1] Xi'an Medical University, Xi'an, China, [2] Department of Hepatobiliary Surgery, Xijing Hospital, The Fourth Military Medical University, Xi'an, China, [3] School of Pharmacy, Health Science Center, Xi'an Jiaotong University, Xi'an, China

**Background:** Hepatocellular carcinoma is one of the most common malignant tumors with a very high mortality rate. The emergence of immunotherapy has brought hope for the cure of hepatocellular carcinoma. Only a small number of patients respond to immune checkpoint inhibitors, and ferroptosis and tertiary lymphoid structure contribute to the increased response rate of immune checkpoint inhibitors; thus, we first need to identify those who are sensitive to immunotherapy and then develop different methods to improve sensitivity for different groups.

**Methods:** The sequencing data of hepatocellular carcinoma from The Cancer Genome Atlas and Gene Expression Omnibus was downloaded to identify the immune-related long non-coding RNAs (lncRNAs). LncRNAs related to survival data were screened out, and a risk signature was established using Cox proportional hazard regression model. R software was used to calculate the riskScore of each patient, and the patients were divided into high- and low-risk groups. The prognostic value of riskScore and its application in clinical chemotherapeutic drugs were confirmed. The relationship between riskScore and immune checkpoint genes, ferroptosis genes, and genes related to tertiary lymphoid structure formation was analyzed by Spearman method. TIMER, CIBERSORT, ssGSEA, and ImmuCellAI were used to evaluate the relative number of lymphocytes in tumor. The Wilcoxon signed-rank test confirmed differences in immunophenoscore between the high- and low-risk groups.

**Results:** Data analysis revealed that our signature could well predict the 1-, 2-, 3-, and 5-year survival rates of hepatocellular carcinoma and to predict susceptible populations with Sorafenib. The risk signature were significantly correlated with immune checkpoint genes, ferroptosis genes, and tertiary lymphoid structure-forming genes, and predicted tumor-infiltrating lymphocyte status. There was a significant difference in IPS scores between the low-risk group and the high-risk group, while the low-risk group had higher scores.

**Conclusion:** The riskScore obtained from an immune-related lncRNA signature could successfully predict the survival time and reflect the efficacy of immune checkpoint

inhibitors. More importantly, it is possible to select different treatments for different hepatocellular carcinoma patients that increase the response rate of immune checkpoint inhibitors and will help improve the individualized treatment of hepatocellular carcinoma.

## INTRODUCTION

Hepatocellular carcinoma (HCC) ranks the fourth in mortality among malignant tumors (1). Viral infection, aflatoxin exposure, smoking, and heavy alcohol consumption are common pathogenic factors leading to HCC (2). Areas including North and West part of Africa and East Southeast part of Asia have a high incidence of HCCs (3, 4). In China, the 5-year survival rate is <14.1% (5). The late onset of symptoms of HCCs makes early diagnosis difficult, and at the time of diagnosis, only one-third of patients are eligible for radical excision (6). The high recurrence rate and short survival time even after surgery indicate the urgent need for the development of precise individualized HCC treatment (7). Compared with traditional treatment, the application of immune checkpoint inhibitors (ICI) (anti-PD1, anti-PD-L1, and anti-CTLA4) has shown better prognostic value in the treatment of several tumors (8–10). At present, nivolumab and pembrolizumab have been used in the clinical treatment of HCC (11). In many cancers therapies, immunotherapy has become a hotspot treatment and is also the most likely treatment plan to achieve long-term survival. The main characteristics of immunotherapy are activation of tumor-infiltrating lymphocytes (TILs), killing of tumor cells, and inhibition of tumor metastasis and recurrence. However, a disadvantage of immunotherapy is that only a few people respond to ICI treatment. Therefore, research on the tumor microenvironment (TME) and tertiary lymphoid structure (TLS) is particularly important (12–14). Understanding the tumor microenvironment, especially TLS, will help boost ICI response rates (14). Only 40% of patients with HCC have TLS. TLS, which refers to the aggregation of lymphocytes in the tumor and at the edge of tumor invasion, has a function similar to lymph node and is an important part of the TME (15). In the future, ICI combined with TLS may be a key way to cure tumors.

Ferroptosis is a newly discovered process of apoptosis, which is closely related to iron metabolism (16). Studies show that ferroptosis can improve the immunotherapy response and inhibit tumor progression (17). ICI combined with ferroptosis-targeted therapy represents a new strategy to prolong the survival time of patients with HCC (18), and it has the potential to cure tumors.

Long non-coding RNAs (lncRNAs) does not have the function of coding protein, and the base length of genome is transcribed into noncoding RNAs, most of which have a great impact on the biological function of cells (19). Different lncRNAs play various roles in cell metabolism, such as promoting cancer growth, suppressing tumor growth, regulating immune responses, and enhancing the tumor infiltrating lymphocytes (20). For example,

lncRNA CYTOR upregulates the expression of oncogene KIAA1522, which in turn affects the proliferation, apoptosis, and cell cycle of HCC cells (21).

The current problem of immunotherapy is that the response rate is low. In the face of this problem, we first need to find out the population with high sensitivity and then develop different methods to improve sensitivity for different groups, so as to achieve the effect of long-term survival or tumor cure. Therefore, we used multiple immune-related lncRNAs (irlncRNAs) from the Cancer Genome Atlas (TCGA) database to solve the problem. Our findings lay the foundation for the precise treatment of HCC so that more patients with HCC can benefit.

## MATERIALS AND METHODS

### Data Download, Preparation, and Screening

HCC transcriptome data and corresponding clinical data were retrieved from the TCGA (https://portal.gdc.cancer.gov/), and immune-related gene sets were obtained from the gene set enrichment analysis (GSEA) (M19817 and M13664) (https://www.gsea-msigdb.org/). The irlncRNAs were identified by Spearman correlation test. Then, irlncRNAs associated with survival time were screened (p < 0.05). Patients with HCC whose survival time was <30 days and whose survival time was uncertain were excluded, leaving data from 343 patients for analysis, and the patients were randomly divided into a training set and a test set. In addition, 59 HCC transcriptome data (GSE40144) from the Gene Expression Omnibus (GEO) database was downloaded (https://www.ncbi.nlm.nih.gov/), as an external validation set.

### Construction of the Signature

LncRNAs associated with survival time were identified by the Cox proportional hazard regression model. The Akaike Information Criterion (AIC) was used to fit the optimal signature. The result with the lowest AIC value was selected to build the signature. RiskScore = expression(A) × cof(A) + expression(B) × cof(B) + …expression(n) × cof(n).

### Test of the Prediction Ability of the Signature

Kaplan–Meier survival curves were used to compare the survival times between the two groups, and multi-index receiver operating characteristic (ROC) curves were drawn to verify the ability of the signature to predict prognosis. Risk curves, survival

status distribution maps, and heatmaps of the risk gene expression profiles were generated to further examine the reliability of the signature.

## Analysis of Clinicopathological Parameters

The pathological parameters were analyzed by Cox regression analysis. At the same time, the Wilcoxon signed-rank test was used to evaluate whether the riskScore was different among the groups of pathological parameters, and the chi-square test was used to analyze the relationship between clinicopathological parameters and the signature.

## Enrichment Analysis

Messenger RNAs (mRNAs) associated with risk genes were screened according to the principle of coexpression, and then STRING was used to analyze the interaction between coexpressed genes (https://string-db.org/). Finally, to understand the carcinogenic mechanism of disease risk genes, R software (4.0.1 version) was used for GO and KEGG pathway enrichment analyses. In addition, we used GSEA software to explore the role of risk genes in immunity (p < 0.05).

## Relationship Between the Signature and Clinical Treatment

To clarify the role of the signature in clinical treatment, the IC50 values of commonly used chemotherapeutic drugs were evaluated using high-throughput sequencing data of HCC in TCGA. The American Joint Committee on Cancer (AJCC) guidelines recommend the use of vincristine, cisplatin, and sorafenib in the treatment of HCC. The Wilcoxon signed-rank test was used to compare the differences between the two groups. Visualization of the results was performed using pRRophetic and ggplot2.

## Analysis of TILs

To determine whether the signature is associated with lymphocyte infiltration, we used the currently recognized online analysis websites TIMER (https://cistrome.shinyapps.io/timer/), CIBERSORT (http://cibersort.stanford.edu/), ssGSEA, and ImmuCellAI (http://bioinfo.life.hust.edu.cn) to calculate the degree of tumor lymphocyte infiltration in each sample. The correlation between the riskScore and TILs was tested by the Spearman test. The CIBERSORT results were used to evaluate the associations among TILs using Spearman analysis.

## Analysis of the Clinical Relevance of Immunotherapy

The immunophenoscore is calculated based on the expression of various important immune molecules in the TME, including major histocompatibility complex (MHC) molecules, immune regulatory factors, effector cells, and suppressor cells, which can well reflect the response rate of ICI. In addition, immune checkpoint gene expression is associated with the response to ICI; therefore, we analyzed the correlation among immune checkpoint genes and the IPS and the signature.

## Analysis of Genes Related to TLS Formation

The TLS helps to improve the immunotherapy response rate, so we explored whether genes related to TLS formation (CCL2, CCL3, CCL4, CCL5, CCL8, CCL18, CCL19, CCL21, CXCL9, CXCL10, CXCL11, CXCL13, and IL7) were associated with the signature.

## Analysis of Ferroptosis-Related Genes

Ferroptosis-related genes were collected from the GSEA database (M39768), and genes associated with survival (p < 0.05) were selected for further analysis.

## Statistical Analysis

All statistical analysis and plots were performed with R (R x64 4.0.3 version; https://www.r-project.org/). A p-value <0.05 was statistically significant. Difference analysis between two groups used Wilcoxon rank sum test. Relation analysis was identified by Spearman correlation analysis. Survival analysis was visualized by K–M curves and determined by log-rank test. Related R packages included "ggplot2," "edgeR," "ggpubr," "survival," "GSEABase," and "GSVA."

# RESULTS

## Identification of Immune-Related LncRNAs Associated With Overall Survival Time
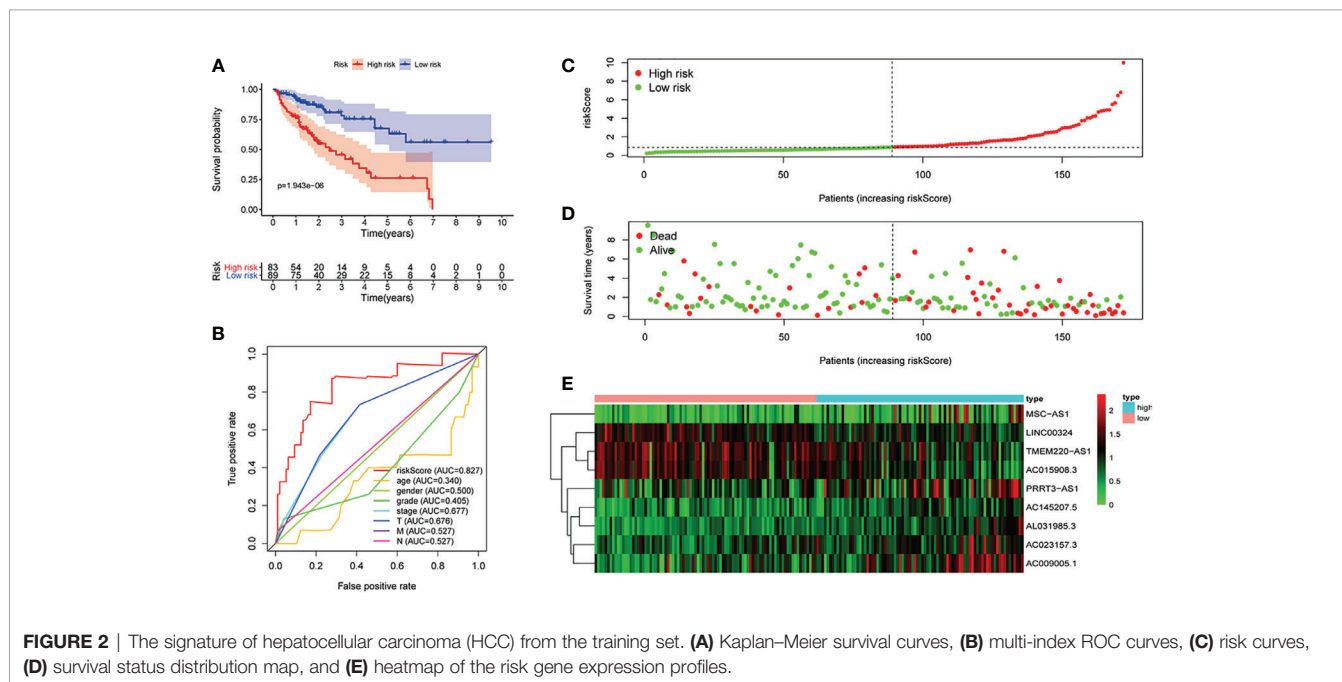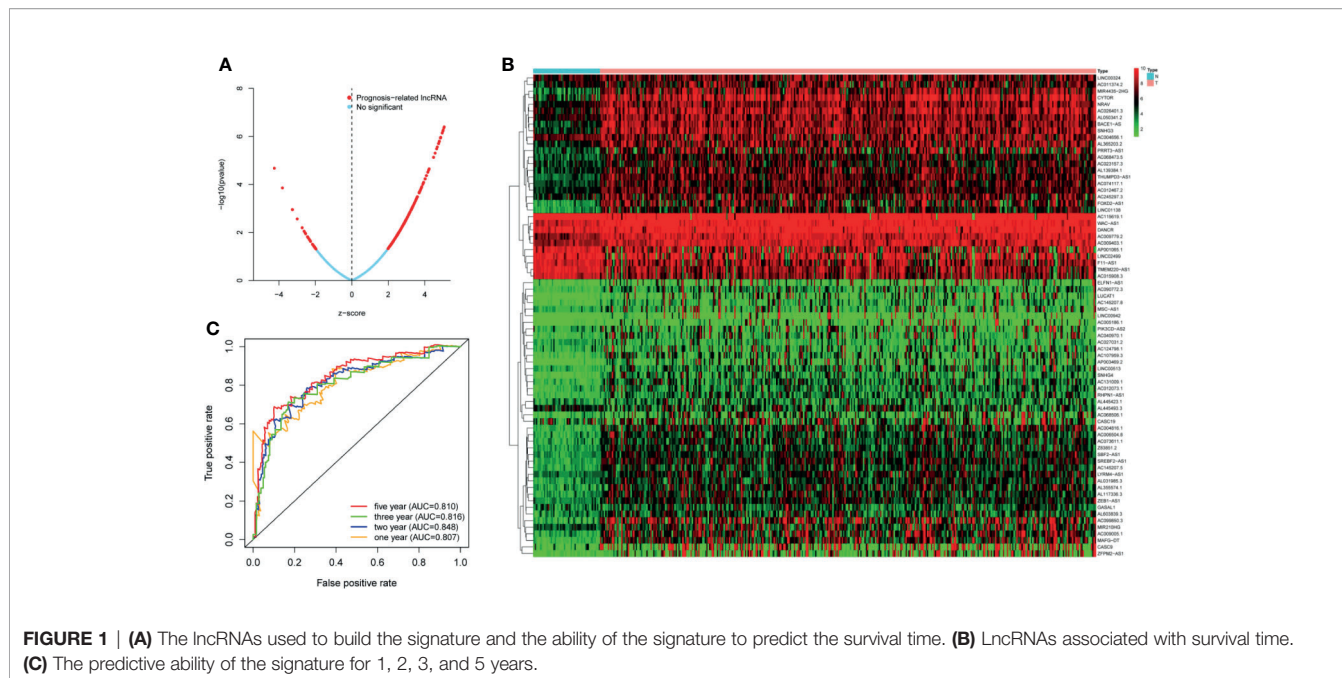
TCGA transcriptome data included 50 normal cases and 374 patients with HCC. A total of 14,121 noncoding RNAs and 19,628 mRNAs were obtained. A total of 1,327 irlncRNAs (R > 0.4, p < 0.001) were obtained by Spearman correlation analysis, of which 250 had significant effects on survival time (p < 0.05) (Figure 1A).

## Signature Identification

We selected 73 irlncRNAs (Figure 1B) associated with survival (p < 0.0002) for Cox proportional hazard regression model screening. Finally, nine differentially expressed genes (LINC00324, MSC-AS1, AC023157.3, AC009005.1 PRRT3-AS1, AC015908.3, AC145207.5, AL031985.3, and TMEM220-AS1) were selected to construct the signature. All patients were randomly divided into high-risk group (172 cases) and low-risk group (171 cases) according to the median value of riskScore calculated by R software.

## Verification of the Prediction Ability of the Signature

First of all, 343 patients were randomly put into a training set (83 high-risk cases and 89 low-risk cases) and a testing set (89 high-risk cases, 82 low-risk cases). Second, the training set (Figures 2A–E), the testing set (Figures 3A–E) and the external validation set (29 high-risk cases, 30 low-risk cases) (Figures 4A–E) were used to generate Kaplan–Meier survival curves, multi-index ROC curves, risk curves, survival status distribution maps, and the heatmaps of risk genes expression profiles. The results of the survival curves showed that patients in
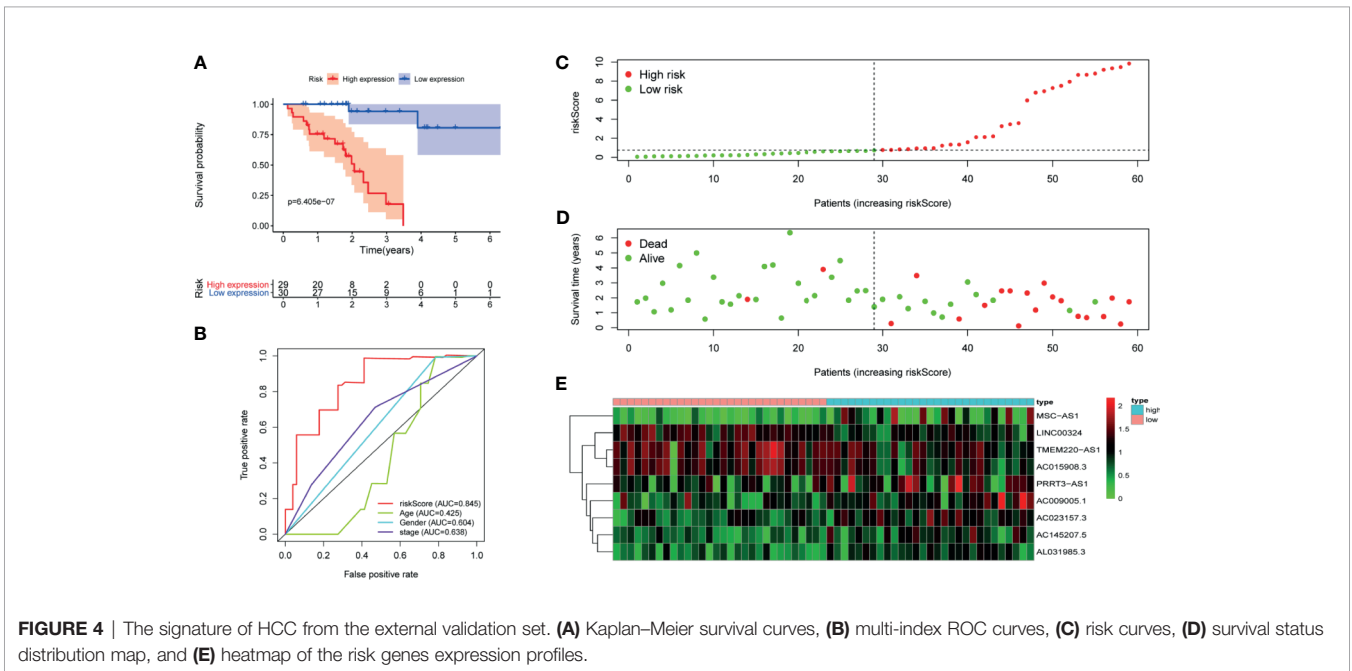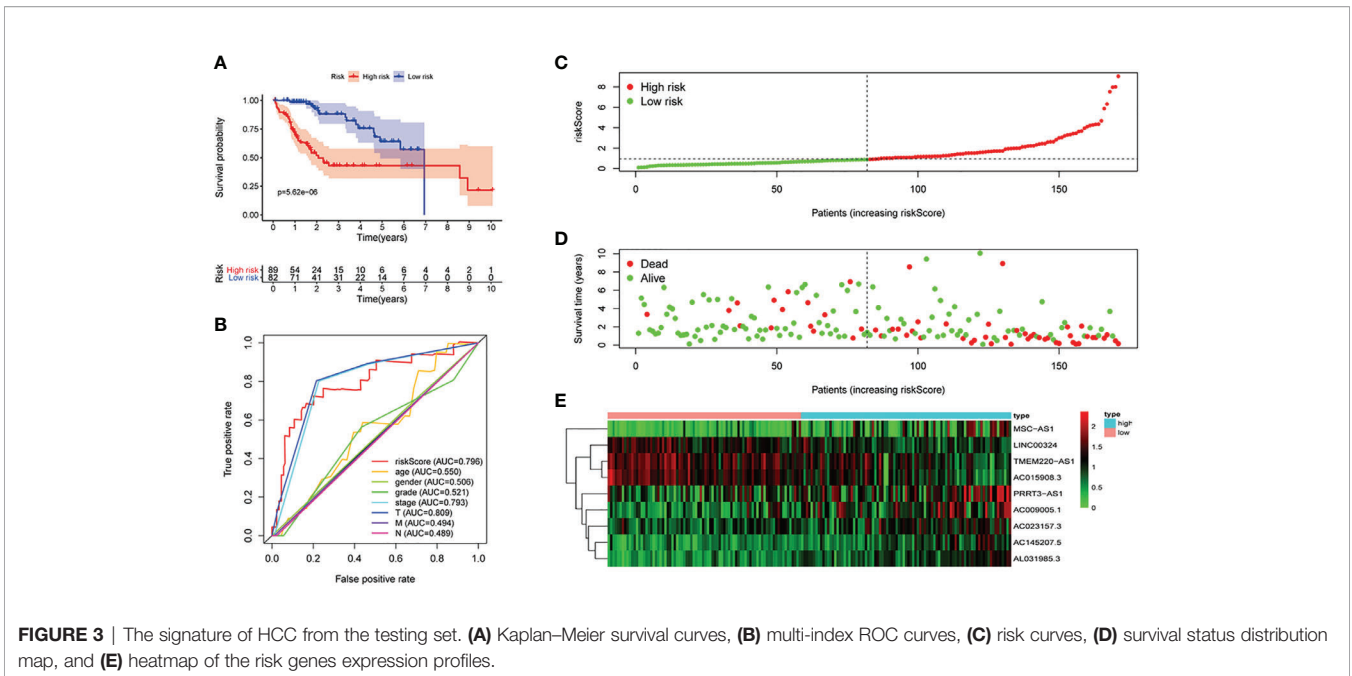
**FIGURE 1** | **(A)** The lncRNAs used to build the signature and the ability of the signature to predict the survival time. **(B)** LncRNAs associated with survival time. **(C)** The predictive ability of the signature for 1, 2, 3, and 5 years.



**FIGURE 2** | The signature of hepatocellular carcinoma (HCC) from the training set. **(A)** Kaplan–Meier survival curves, **(B)** multi-index ROC curves, **(C)** risk curves, **(D)** survival status distribution map, and **(E)** heatmap of the risk gene expression profiles.

the low-risk group had significantly longer overalls survival time. The comparison of the area under the multi-index ROC curve revealed that the riskScore was better able to predict survival time than the traditional stage-by-stage method. Finally, to verify whether the signature was applicable to both the early and late stages of HCC, we drew the corresponding survival curves for both stages (**Figures 5A, B**). The results show that the high-risk group has significant difference with the low-risk group in survival time. In addition, areas under the ROC curve (AUCs)

at 1 year (AUC = 0.807), 2 years (AUC = 0.848), 3 years (AUC = 0.816), and 5 years (AUC = 0.810) (**Figure 1C**) demonstrated the strong ability of the signature in predicting survival time. All of the above results showed that our signature has a high application value and reliability.

## Pathological Parameter Analysis

Cox regression analysis was used to analyze clinicopathological parameters (age, gender, survival status, grade, stage, T, N, M).

**FIGURE 3** | The signature of HCC from the testing set. **(A)** Kaplan–Meier survival curves, **(B)** multi-index ROC curves, **(C)** risk curves, **(D)** survival status distribution map, and **(E)** heatmap of the risk genes expression profiles.



**FIGURE 4** | The signature of HCC from the external validation set. **(A)** Kaplan–Meier survival curves, **(B)** multi-index ROC curves, **(C)** risk curves, **(D)** survival status distribution map, and **(E)** heatmap of the risk genes expression profiles.

The results are shown in **Table 1**. In addition, we used the chi-square test to verify the correlation between clinicopathological parameters and the riskScore (**Figure 6A**, ***p < 0.001, **p < 0.01, and *p < 0.05). Survival status, grade, stage, gender, and T stage were highly correlated to the riskScore, which was an independent prognostic factor. Then, to explore the difference in riskScores between different groups, we used the Wilcoxon signed-rank test. Results are presented in **Figures 6B–F**.

## Enrichment Analysis

Exploring the biological functions of risk genes is helpful to understand their potential molecular mechanisms in tumorigenesis and development and can provide new targets for the treatment of HCC. According to the principle of coexpression, a total of 606 genes associated with risk genes (R > 0.4, p < 0.05) were identified, of which 604 were significantly differentially expressed. First, the significantly differentially expressed genes with a correlation coefficient >0.99 were selected for visualization
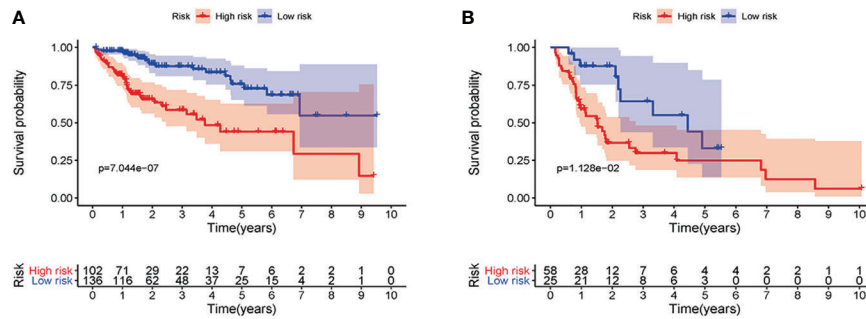
**FIGURE 5** | **(A)** Survival curve of early patients and **(B)** survival curve of advanced patients.

**TABLE 1** | Univariate and multivariate Cox regression analyses in each patient set.

| Variables | Univariate analysis | | Multivariate analysis | |
|---|---|---|---|---|
| | HR (95% CI) | p-value | HR (95% CI) | p-value |
| **Training set** | | | | |
| Age | 0.98 (0.95,1.01) | 0.14 | | |
| Gender | 1.01 (0.48,2.14) | 0.98 | | |
| Grade | 0.81 (0.50,1.32) | 0.40 | | |
| Stage | 1.55 (1.06,6.26) | 0.02 | | |
| T | 1.49 (1.04,2.14) | 0.03 | | |
| M | 6.66 (1.55,28.58) | 0.01 | | |
| N | 2.42 (0.33,17.90) | 0.390 | | |
| riskScore | 1.52 (1.30,1.78) | 9.84E−08 | 1.61 (1.33,1.95) | 1.16E−06 |
| **Testing set** | | | | |
| Age | 1.01 (0.99,1.04) | 0.35 | | |
| Gender | 0.59 (0.31,1.14) | 0.12 | | |
| Grade | 1.20 (0.78,1.86) | 0.40 | | |
| Stage | 2.66 (1.83,3.88) | 3.46E−07 | | |
| T | 2.50 (1.79,3.50) | 9.42E−08 | | |
| M | 2.25 (0.31,16.59) | 0.43 | | |
| N | 1.37 (0.19,10.04) | 0.76 | | |
| riskScore | 1.36 (1.22,1.51) | 4.51E−08 | 1.28 (1.14,1.45) | 6.06E−05 |
| **External validation set** | | | | |
| Age | 0.75 (0.29,1.93) | 0.55 | | |
| Gender | 1.07 (0.86,4.92) | 0.07 | | |
| Stage | 1.67 (1.15,4.25) | 0.03 | 3.02 (1.02,8.90) | 0.04 |
| riskScore | 4.51 (2.13,6.37) | 0 | 5.53 (4.13,6.37) | 0 |

(**Figure 7A**). The molecules CDC20, NOP56, SNRPG, SNRPF, BUB1B, and BMS1 were at the core of the protein interaction network. Second, to understand the carcinogenic mechanism of risk genes, coexpressed proteins were subjected to enrichment analysis. The results of Gene Ontology (GO) database enrichment analysis are shown in **Figures 8A, B**. The outcomes of the Kyoto Encyclopedia of Genes and Genomes (KEGG) database enrichment analysis are shown in **Figures 8C, D**. The results (**Figure 7B**) of GSEA suggested the importance of the risk genes for immune pathway regulation and showed that the high-risk group was in a state of immunosuppression.

## Application of the Signature in Clinical Treatment

The results of the IC50 analysis of chemotherapeutic drugs are shown in **Figure 9**. The low-risk group showed a better response to sorafenib, but there was no significant difference in the response to vincristine or cisplatin.

## Analysis of TILs

LncRNAs regulate immune-related genes that affect the TILs, which are terminal targets of ICI. Therefore, we explored whether there was a correlation between TILs and the riskScore. Results of CIBERSORT, TIMER, ImmuCellAI, and ssGSEA are shown in **Figure 10A**. Exhausted cells, macrophages, myeloid-derived suppressor cells (MDSCs), Treg cells, neutrophils, and eosinophils were positively correlated with the riskScore. Negative correlations were observed among Th17 cells, CD8+ T cells, cytotoxic T cells, NK cells, and mucosal-associated invariant T (MAIT) cells with the riskScore. In addition, the CIBERSORT analysis results showed a correlation among lymphocytes (**Figure 10B**). There was a weak to moderate correlation among various lymphocytes in the TME.
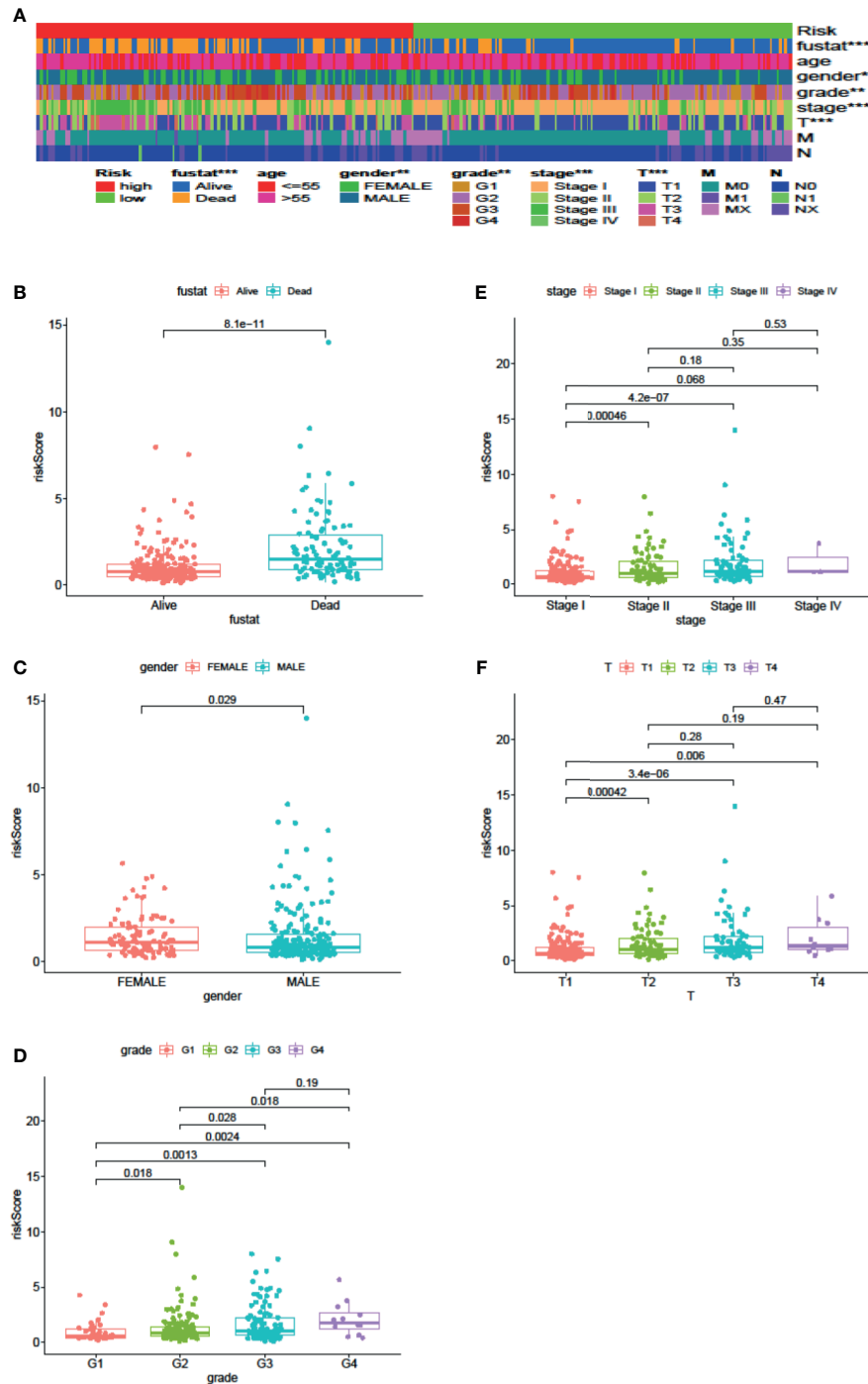
**FIGURE 6** | Clinical Evaluation by the Signature. A strip chart **(A)** along with the scatter diagram showed that survival status **(B)**, gender **(C)**, tumor grade **(D)**, clinical stage **(E)**, and T stage **(F)** were significantly associated with the riskScore (P <0.001 = ***, P <0.01 = **, and P <0.05 = *).

## Immunotherapy Analysis

The clinical application of ICI benefits many tumor patients, so we analyzed the relationships among immune checkpoint genes, immunophenoscore (IPS), and the signature. Our study found out that a riskScore was positively correlated with CD276,

SIRPA, CD47, TNFRSF14, PDCD1, CTLA4, TIGIT, LGALS9, HAVCR2, CD86, CD274, CD80, and PVR expression (**Figure 10C**). The IPS analysis showed that the scores of IPS, IPS–PD1 blocker, IPS–CTLA4 blocker, and IPS–PD1–CTLA4 blocker scores were higher in the low-risk group (**Figure 10D**).
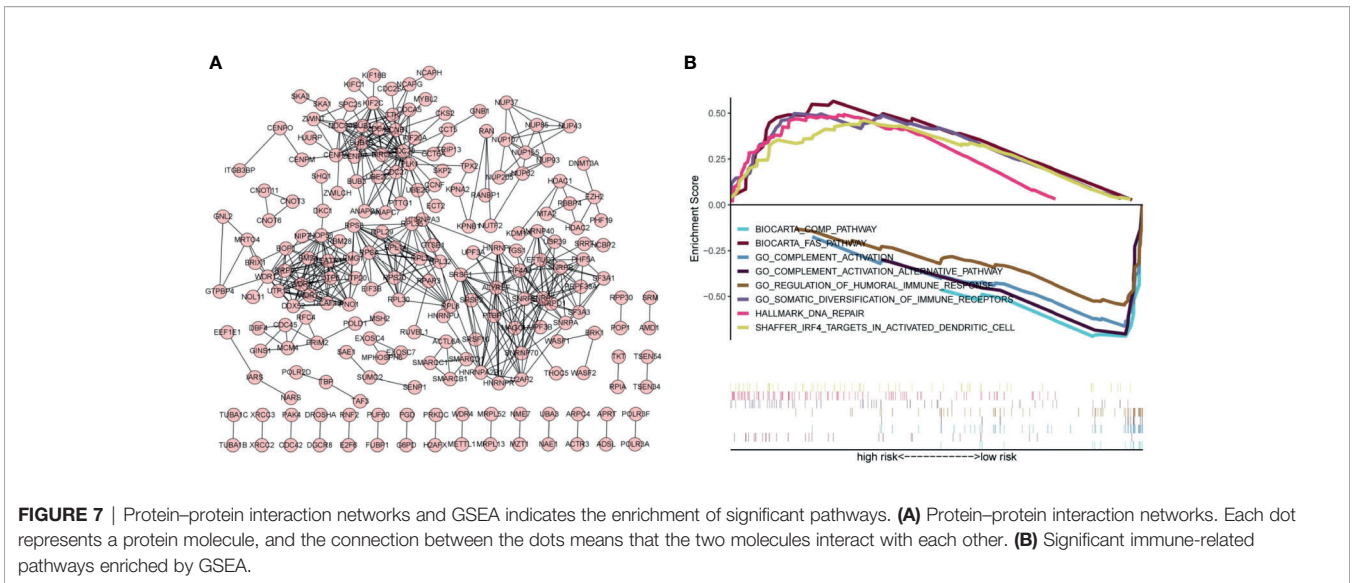
**FIGURE 7** | Protein–protein interaction networks and GSEA indicates the enrichment of significant pathways. **(A)** Protein–protein interaction networks. Each dot represents a protein molecule, and the connection between the dots means that the two molecules interact with each other. **(B)** Significant immune-related pathways enriched by GSEA.
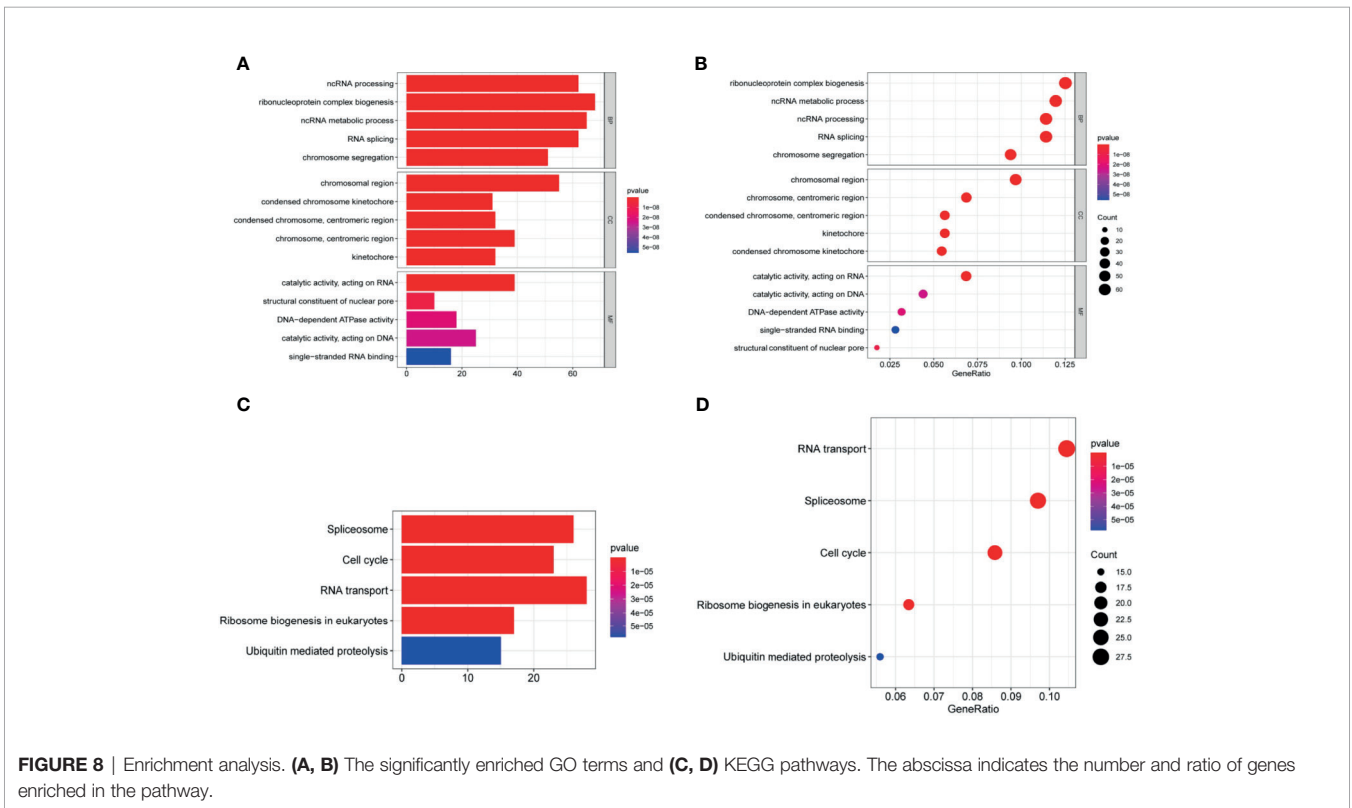


**FIGURE 8** | Enrichment analysis. **(A, B)** The significantly enriched GO terms and **(C, D)** KEGG pathways. The abscissa indicates the number and ratio of genes enriched in the pathway.

## Exploring Tertiary Lymphoid Structure-Related Genes

The TLS, an important part of the TME, has the ability to enhance the immune response to treatment. The genes related to TLS formation of CCL2, CCL3, CCL4, CCL5, CCL8, CCL19, CCL21, CXCL10, CXCL13, and IL7 were positively correlated with the riskScore (**Figure 11A**). Negative correlations were observed among CCL18, CXCL9, and CXCL11 with the

riskScore. The data showed that the high risk group was genetically predisposed to form TLS, so the patients in the high-risk group were more likely to achieve a high response rate of immunotherapy through TLS in the future.
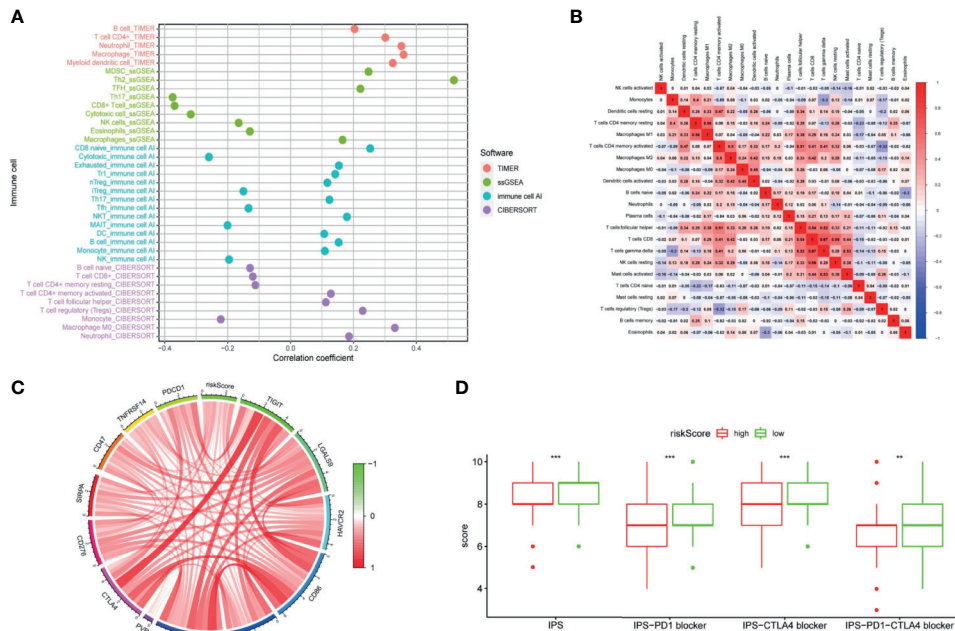
## Analysis of Ferroptosis-Related Genes

Previous studies have shown that ferroptosis increases the response to immunotherapy to enhance efficacy and inhibit
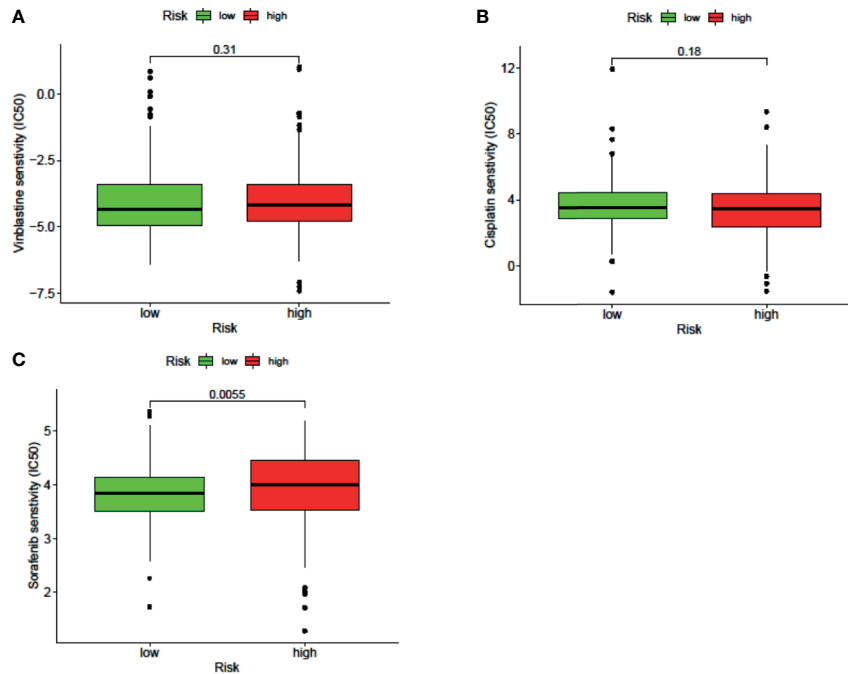
**FIGURE 9** | The signature can be used as a potential indicator to predict the sensitivity to sorafenib, and the sorafenib IC50 was higher in the high-risk group.



**FIGURE 10** | The signature was used to evaluate tumor-infiltrating lymphocytes, immunophenoscore (IPS), and immune checkpoint genes. **(A)** Spearman correlation analysis was used to calculate the correlation between the riskScore and the number of tumor-infiltrating lymphocytes. **(B)** Correlation heatmap of 22 tumor-infiltrating lymphocytes. **(C)** Analysis of the correlation between the riskScore and immune checkpoint genes. **(D)** The IPS, IPS-PD1 blocker, IPS–CTLA4 blocker, and IPS–PD1–CTLA4 blocker values are higher in the low risk group. (P <0.001 = *** and P <0.01 = **).
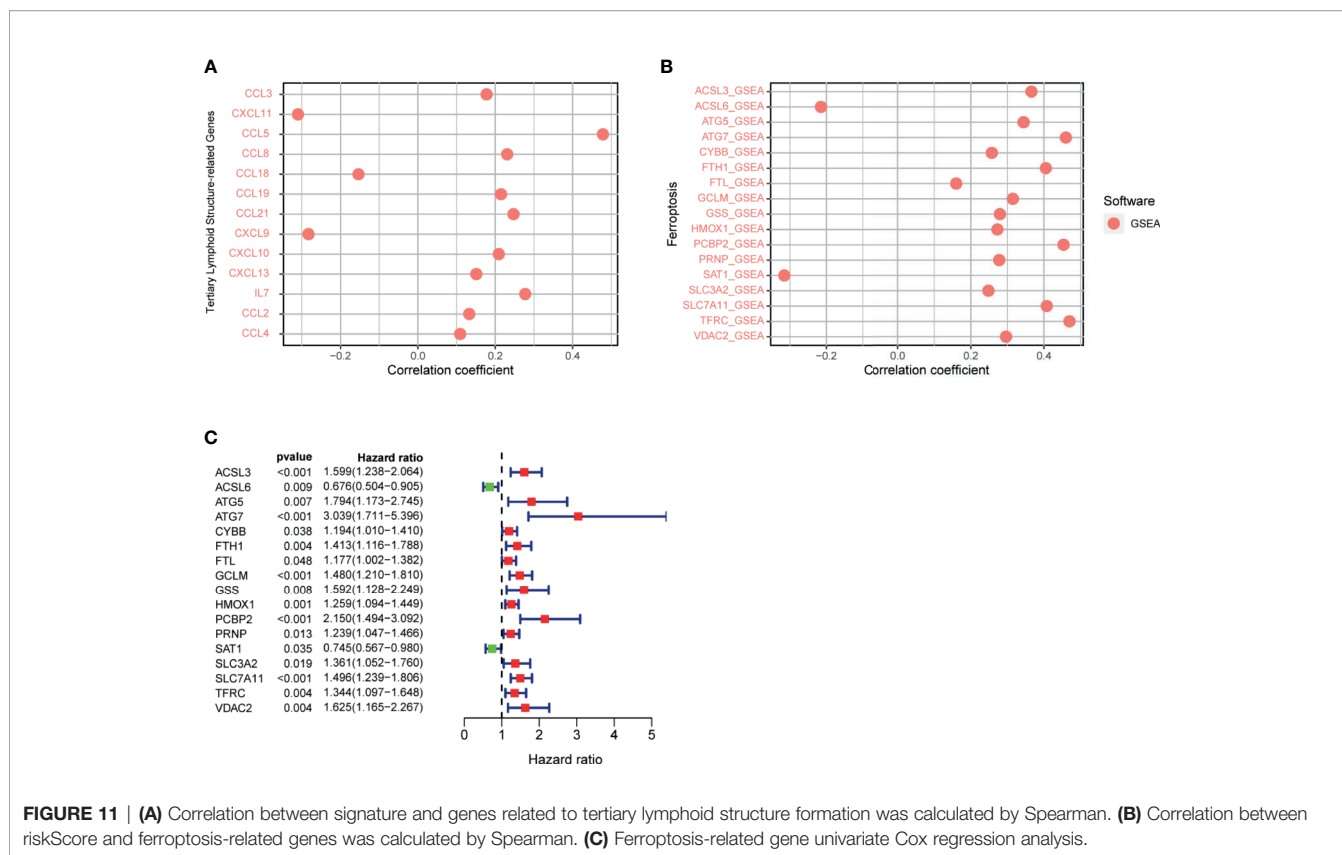
**FIGURE 11** | **(A)** Correlation between signature and genes related to tertiary lymphoid structure formation was calculated by Spearman. **(B)** Correlation between riskScore and ferroptosis-related genes was calculated by Spearman. **(C)** Ferroptosis-related gene univariate Cox regression analysis.

tumor progression. Therefore, we analyzed the correlation between the signature and ferroptosis-related genes, which presented a positive correlation between the riskScore and the expression of ACSL3, ATG5, ATG7, CYBB, FTH1, FTL, GCLM, GSS, HMOX1, PCBP2, PRNP, SLC3A2, SLC7A11, TFRC, and VDAC2, respectively (**Figure 11B**). However, the expression of ACSL6 and SAT1 were negatively correlated with the riskScore, respectively. The above analysis revealed that the greater the riskScore, the weaker the degree of ferroptosis. The results of the COX univariate analysis of ferroptosis-related genes are shown in **Figure 11C**.

## DISCUSSION

Increasing evidence demonstrated that lncRNAs seriously affect the occurrence, development, and metastasis of HCC and play an indispensable part in TME's regulation process (22–24). The TME is not only related to the occurrence and development of cancers but also highly related to the response to ICI (25). At present, among the many treatment schemes for HCC, immunotherapy is the most popular choice and the most likely new therapy to make a considerable difference in patient outcomes. The future of HCC treatment is likely to involve immunotherapy combined with targeted therapy (26, 27). The postoperative recurrence and mortality rates of patients with HCC are high; the effective rate of ICI therapy is low. Our

signature cannot only identify people who are sensitive to ICI but also select different methods to improve the response rate of ICI for different populations.

LINC00324 regulates FasL and PU.1 to promote the biological behavior proliferation, invasion, metastasis, and apoptosis of HCC stem cells (28). PRRT3-AS1 controls the mTOR signaling pathway to promote the invasion and metastasis and inhibits the autophagy and apoptosis of prostate cancer cells (29). MSC-AS1 induces PGK1 expression and accelerates the progression of HCC (30). In addition, MSC-AS1 has a similar role in gliomas (31), gastric cancer (32), renal clear cell carcinoma (33), and pancreatic cancer (34). TMEM220-AS1, AC015908.3, AC009005.1, and AL031985.3 have been reported in a signature predictive of overall survival. AC145207.5 and AC023157.3 are reported here for the first time. The survival curve was generated by the riskScore, and the results showed that the high-risk group has a significantly lower overall survival rate than the low-risk group. To validate the predictive ability of the signature, the areas under the ROC curve were calculated as AUC(1 year) = 0.807, AUC(2 year) = 0.848, AUC(3 year) = 0.816, and AUC(5 year) = 0.810, suggesting that the ability of our signature to predict overall survival was accurate and fines. Cox univariate and multivariate analyses revealed that the riskScore was an independent prognostic factor.

Better understanding of the TME will help develop new methods to modify the TME or treat HCC resulting in improving the response rate and efficacy of immunotherapy (35).

At the same time, it will lay a solid foundation for the future implementation of immunotherapy combined targeted therapy. ICI rely on TILs against tumor cells. Therefore, we used CIBERSORT (36), ImmuCellAI (37), TIMER (38), and ssGSEA (39) to evaluate the relative number of TILs in each patient. As we expected, some of the lymphocytes showed differences between the two groups. Exhausted cells, macrophages, Treg cells, neutrophils, MDSCs, and eosinophils were more common in the high-risk group, while CD8+ T cells, cytotoxic T cells, natural killer (NK) cells, Th17 cells, and MAIT cells were more common in the low-risk group. Studies have found that the exhausted cells have a positive impact on the poor prognosis, and the completely exhausted CD8+ T cells do not respond to ICI (40, 41). Macrophages could increase the proliferation of HCC stem cells through the IL-6/STAT3 signaling pathway and then promote tumor growth (42). Treg cells regulate the expression of CTLA-4, PD-1, and TGF-β to directly bind with the corresponding receptors on target cells and inhibit the expression of the important cytokines interferon-gamma (IFN-γ), tumor necrosis factor-α (TNF-α), and IL-2 that affect T cells. In addition, tumor cells regulate chemokine receptor 28 (CCL28), thus recruiting Treg cells, enhancing the immune tolerance, and promoting the angiogenesis (43). The migration of neutrophils to tumors is mainly mediated by CXC chemokine binding to CXCR1 and CXCR2, which can promote tumor growth, invasion, angiogenesis, and metastasis (44). CD8+ T cells are positively correlated not only with good prognosis but also with the ICI response. Cytotoxic T cells specifically recognize the endogenous peptide MHC I complexes and kill tumor cells by expressing FasL or secreting TNF-α (43). The number of tumor-infiltrating NK cells positively correlated with the prognosis of HCC patients (45). Our results support the above conclusions. Considerable evidence shows that the TME is a whole, and all kinds of lymphocytes in the TME interact with each other (46). Our research results are consistent with this view. Therefore, the accuracy of analysis of the prognostic value of a certain type of cells alone is far lower than that of a combined multicell analysis. Studies that focus only on a specific kind of lymphocyte provide only a one-sided understanding of the TME and which cannot achieve a comprehensive, let alone a real, understanding of the TME. There were relatively few CD8+ T cells in the high-risk group, which may be one of reasons why more dendritic cells and shorter overall survival times were associated with the high-risk group. Moreover, our research found that there were more immunosuppressive cells and evading immune surveillance signals in the high-risk group, while more immune-enhancing cells and complement activation signals were found in the low-risk group. These observations revealed that the low-risk group is characterized by the immune activity and the inhibition of tumor progression. It also partially explained why the high-risk group is in a state of immunosuppression.

It has been reported that the IPS is a good predictor for the response of ICI (47), so we investigated the correlation between the IPS and the riskScore. IPS, IPS–PD1 blocker, IPS–CTLA4 blocker, and IPS–PD1–CTLA4 blocker were significantly higher in the low-risk group, indicating that the riskScore is the representative immunogenicity of TME in HCC. Higher gene expression level of immune checkpoint is one of the causes of an immunosuppressive state. According to a previous investigation, the anti-CTLA4 and anti-PD-1 treatment reactivated the antitumor immune response in the TME of HCC (48), and the expression of immune checkpoint genes was associated with the response to ICI (8). Our results demonstrated that the expression levels of CD276, SIRPA, CD47, TNFRSF14, PDCD1, CTLA4, TIGIT, LGALS9, HAVCR2, CD86, CD274, CD80, and PVR increased in the high risk group. The above results showed that the low-risk group of patients is more sensitive to treatment with ICI.

Only about 40% of patients with HCC have TLS within the tumor. Recent studies have reported that TLS, which have a similar function to the lymph node, enhance the sensitivity to ICI therapy (6). Therefore, the relationship between the molecules related to the formation of TLS and the signature was analyzed. Genes related to the formation of TLS, including CCL2, CCL3, CCL4, CCL5, CCL8, CCL19, CCL21, CXCL10, CXCL13, and IL7, were positively correlated with the riskScore, which indicated that patients in the high-risk group had a genetic advantage informing TLS. In the future, combining ICI with tertiary lymphoid structure-targeting therapy may improve the prognosis of patients; this gives patients who are not sensitive to ICI the opportunity to cure their tumors.

Ferroptosis enhances the effectiveness of ICI and inhibits the tumor progression (17). The expression of IFN-γ regulatory system X-c secreted by cytotoxic T cells enhances the sensitivity to ferroptosis (16). This suggests that ICI combined with ferroptosis inducers may become a new strategy for the treatment of cancer in the future. We analyzed 17 ferroptosis genes associated with the prognosis of HCC, of which 15 were positively correlated with the riskScore and 2 were negatively correlated. This suggests that the signature is fully capable of predicting tumor sensitivity to ferroptosis. In addition, in our study, the proportion of cytotoxic T cells in the low-risk group was significantly higher than that in the high-risk group. All this evidence suggests that patients in the low-risk group were not only more sensitive to ICI but also likely to be cured of their tumors by targeting ferroptosis in combination with immunotherapy.

It is important to recognize the shortcomings of the signature developed in this study: in clinical practice, screening out different treatments based on riskScore does not simply divide into high- and low-expression groups but requires more detailed subdivision. In future work, we need to collect more data to further verify the reliability of the findings.

## DATA AVAILABILITY STATEMENT

The data presented in the study are deposited in the FigShare repository, accession link: https://figshare.com/s/93afe076e2ed13d32f4d.

## AUTHOR CONTRIBUTIONS

WJS and YN conceived of and designed the study. YN, JHL, WLW, DNG and WJS performed the literature search, generated the figures and tables, and wrote the manuscript. JHL, WLW,

XJL, TCZ, ZZM and YFW collected and analyzed the data, and critically reviewed the manuscript. WJS, YN, and DNG supervised the study and reviewed the manuscript. All authors contributed to the article and approved the submitted version.

## FUNDING

## REFERENCES

1. Allemani C, Matsuda T, Di Carlo V, Harewood R, Matz M, Nikšić M, et al. Global Surveillance of Trends in Cancer Survival 2000-14 (CONCORD-3): Analysis of Individual Records for 37 513 025 Patients Diagnosed With One of 18 Cancers From 322 Population-Based Registries in 71 Countries. *Lancet* (2018) 391:1023–75. doi: 10.1016/S0140-6736(17)33326-3

2. Cui Y, Liang S, Zhang S, Zhang C, Zhao Y, Wu D, et al. ABCA8 Is Regulated by miR-374b-5p and Inhibits Proliferation and Metastasis of Hepatocellular Carcinoma Through the ERK/ZEB1 Pathway. *J Exp Clin Cancer Res* (2020) 39:90. doi: 10.1186/s13046-020-01591-1

3. El-Serag HB, Rudolph KL. Hepatocellular Carcinoma: Epidemiology and Molecular Carcinogenesis. *Gastroenterol* (2007) 132:2557–76. doi: 10.1053/j.gastro.2007.04.061

4. Stockdale AJ, Chaponda M, Beloukas A, Phillips RO, Matthews PC, Papadimitropoulos A, et al. Prevalence of Hepatitis D Virus Infection in Sub-Saharan Africa: A Systematic Review and Meta-Analysis. *Lancet Glob Health* (2017) 5:e992–1003. doi: 10.1016/S2214-109X(17)30298-X

5. Sung H, Ferlay J, Siegel RL, Laversanne M, Soerjomataram I, Jemal A, et al. Global Cancer Statistics 2020: GLOBOCAN Estimates of Incidence and Mortality Worldwide for 36 Cancers in 185 Countries. *CA Cancer J Clin* (2021) 71:209–49. doi: 10.3322/caac.21660

6. Calderaro J, Petitprez F, Becht E, Laurent A, Hirsch TZ, Rousseau B, et al. Intra-Tumoral Tertiary Lymphoid Structures Are Associated With a Low Risk of Early Recurrence of Hepatocellular Carcinoma. *J Hepatol* (2019) 70:58–65. doi: 10.1016/j.jhep.2018.09.003

7. Zhou J, Yu L, Gao X, Hu J, Wang J, Dai Z, et al. Plasma microRNA Panel to Diagnose Hepatitis B Virus-Related Hepatocellular Carcinoma. *J Clin Oncol* (2011) 29:4781–8. doi: 10.1200/JCO.2011.38.2697

8. Motzer RJ, Escudier B, McDermott DF, George S, Hammers HJ, Srinivas S, et al. Nivolumab Versus Everolimus in Advanced Renal-Cell Carcinoma. *N Engl J Med* (2015) 373:1803–13. doi: 10.1056/NEJMoa1510665

9. Postow MA, Chesney J, Pavlick AC, Robert C, Grossmann K, McDermott D, et al. Nivolumab and Ipilimumab Versus Ipilimumab in Untreated Melanoma. *N Engl J Med* (2015) 372:2006–17. doi: 10.1056/NEJMoa1414428

10. Slater RL, Lai Y, Zhong Y, Li H, Meng Y, Moreno BH, et al. The Cost Effectiveness of Pembrolizumab Versus Chemotherapy or Atezolizumab as Second-Line Therapy for Advanced Urothelial Carcinoma in the United States. *J Med Econ* (2020) 23:967–77. doi: 10.1080/13696998.2020.1770261

11. Longo V, Brunetti O, Gnoni A, Licchetta A, Delcuratolo S, Memeo R, et al. Emerging Role of Immune Checkpoint Inhibitors in Hepatocellular Carcinoma. *Med (Kaunas)* (2019) 55:698. doi: 10.3390/medicina55100698

12. Zhang B, Wu Q, Li B, Wang D, Wang L, Zhou YL. M6a Regulator-Mediated Methylation Modification Patterns and Tumor Microenvironment Infiltration Characterization in Gastric Cancer. *Mol Cancer* (2020) 19:53. doi: 10.1186/s12943-020-01170-0

13. Petitprez F, de Reyniès A, Keung EZ, Chen TW, Sun CM, Calderaro J, et al. B Cells Are Associated With Survival and Immunotherapy Response in Sarcoma. *Nature* (2020) 577:556–60. doi: 10.1038/s41586-019-1906-8

14. Salem D, Chelvanambi M, Storkus WJ, Fecek RJ. Cutaneous Melanoma: Mutational Status and Potential Links to Tertiary Lymphoid Structure Formation. *Front Immunol* (2021) 12:629519. doi: 10.3389/fimmu.2021.629519

15. Li H, Wang J, Liu H, Lan T, Xu L, Wang G, et al. Existence of Intratumoral Tertiary Lymphoid Structures Is Associated With Immune Cells Infiltration and Predicts Better Prognosis in Early-Stage Hepatocellular Carcinoma. *Aging (Albany NY)* (2020) 12:3451–72. doi: 10.18632/aging.102821

16. Zhou B, Liu J, Kang R, Klionsky DJ, Kroemer G, Tang D. Ferroptosis Is a Type of Autophagy-Dependent Cell Death. *Semin Cancer Biol* (2020) 66:89–100. doi: 10.1016/j.semcancer.2019.03.002

17. Wang W, Green M, Choi JE, Gijón M, Kennedy PD, Johnson JK, et al. CD8+ T Cells Regulate Tumour Ferroptosis During Cancer Immunotherapy. *Nature* (2019) 569:270–4. doi: 10.1038/s41586-019-1170-y

18. Wu Y, Yu C, Luo M, Cen C, Qiu J, Zhang S, et al. Ferroptosis in Cancer Treatment: Another Way to Rome. *Front Oncol* (2020) 10:571127. doi: 10.3389/fonc.2020.571127

19. Zhang L, Xu X, Su X. Noncoding RNAs in Cancer Immunity: Functions, Regulatory Mechanisms, and Clinical Application. *Mol Cancer* (2020) 19:48. doi: 10.1186/s12943-020-01154-0

20. Chen YG, Satpathy AT, Chang HY. Gene Regulation in the Immune System by Long Noncoding RNAs. *Nat Immunol* (2017) 18:962–72. doi: 10.1038/ni.3771

21. Hu B, Yang XB, Yang X, Sang XT. LncRNA CYTOR Affects the Proliferation, Cell Cycle and Apoptosis of Hepatocellular Carcinoma Cells by Regulating the miR-125b-5p/KIAA1522 Axis. *Aging (Albany NY)* (2020) 13:2626–39. doi: 10.18632/aging.202306

22. Hu Y, Zhang X, Zai HY, Jiang W, Xiao L, Zhu Q. lncRNA DUXAP8 Facilitates Multiple Malignant Phenotypes and Resistance to PARP Inhibitor in HCC via Upregulating Foxm1. *Mol Ther Oncolytics* (2020) 19:308–22. doi: 10.1016/j.omto.2020.10.010

23. Hu ZQ, Li HC, Teng F, Chang QM, Wu XB, Feng JF, et al. Long Noncoding RNA MAFG-AS1 Facilitates the Progression of Hepatocellular Carcinoma via Targeting miR-3196/OTX1 Axis. *Eur Rev Med Pharmacol Sci* (2020) 24:12131–43. doi: 10.26355/eurrev_202012_24002

24. Atianand MK, Caffrey DR, Fitzgerald KA. Immunobiology of Long Noncoding RNAs. *Annu Rev Immunol* (2017) 35:177–98. doi: 10.1146/annurev-immunol-041015-055459

25. Peng X, He Y, Huang J, Tao Y, Liu S. Metabolism of Dendritic Cells in Tumor Microenvironment: For Immunotherapy. *Front Immunol* (2021) 12:613492. doi: 10.3389/fimmu.2021.613492

26. Shigeta K, Datta M, Hato T, Kitahara S, Chen IX, Matsui A, et al. Dual Programmed Death Receptor-1 and Vascular Endothelial Growth Factor Receptor-2 Blockade Promotes Vascular Normalization and Enhances Antitumor Immune Responses in Hepatocellular Carcinoma. *Hepatology* (2020) 71:1247–61. doi: 10.1002/hep.30889

27. Yang Y, Wang C, Sun H, Jiang Z, Zhang Y, Pan Z. Apatinib Prevents Natural Killer Cell Dysfunction to Enhance the Efficacy of Anti-PD-1 Immunotherapy in Hepatocellular Carcinoma. *Cancer Gene Ther* (2021) 28:89–97. doi: 10.1038/s41417-020-0186-7

28. Gao J, Dai C, Yu X, Yin XB, Zhou F. Long Noncoding RNA LINC00324 Exerts Protumorigenic Effects on Liver Cancer Stem Cells by Upregulating Fas Ligand *via* PU Box Binding Protein. *FASEB J* (2020) 34:5800–17. doi: 10.1096/fj.201902705RR

29. Fan L, Li H, Wang W. Long Non-Coding RNA PRRT3-AS1 Silencing Inhibits Prostate Cancer Cell Proliferation and Promotes Apoptosis and Autophagy. *Exp Physiol* (2020) 105:793–808. doi: 10.1113/EP088011

30. Cao C, Zhong Q, Lu L, Huang B, Li J, Meng L, et al. Long Noncoding RNA MSC-AS1 Promotes Hepatocellular Carcinoma Oncogenesis via Inducing the Expression of Phosphoglycerate Kinase 1. *Cancer Med* (2020) 9:5174–84. doi: 10.1002/cam4.3080

31. Li C, Feng S, Chen L. MSC-AS1 Knockdown Inhibits Cell Growth and Temozolomide Resistance by Regulating miR-373-3p/CPEB4 Axis in Glioma Through PI3K/Akt Pathway. *Mol Cell Biochem* (2021) 476:699–713. doi: 10.1007/s11010-020-03937-x

32. Jin X, Qiao L, Fan H, Liao C, Zheng J, Wang W, et al. Long Non-Coding RNA MSC-AS1 Facilitates the Proliferation and Glycolysis of Gastric Cancer Cells by Regulating PFKFB3 Expression. *Int J Med Sci* (2021) 18:546–54. doi: 10.7150/ijms.51947

33. Hu Z, Li L, Cheng P, Liu Q, Zheng X, Peng F, et al. lncRNA MSC-AS1 Activates Wnt/β-Catenin Signaling Pathway to Modulate Cell Proliferation

and Migration in Kidney Renal Clear Cell Carcinoma *via* miR-3924/WNT5A. *J Cell Biochem* (2020) 121:4085–93. doi: 10.1002/jcb.29594

34. Sun Y, Wang P, Yang W, Shan Y, Zhang Q, Wu H. The Role of lncRNA MSC-AS1/miR-29b-3p Axis-Mediated CDK14 Modulation in Pancreatic Cancer Proliferation and Gemcitabine-Induced Apoptosis. *Cancer Biol Ther* (2019) 20:729–39. doi: 10.1080/15384047.2018.1529121

35. Dai Y, Qiang W, Lin K, Gui Y, Lan X, Wang D. An Immune-Related Gene Signature for Predicting Survival and Immunotherapy Efficacy in Hepatocellular Carcinoma. *Cancer Immunol Immunother* (2021) 70:967–79. doi: 10.1007/s00262-020-02743-0

36. Wang L, Yang Z, Cao Y. Regulatory T Cell and Activated Natural Killer Cell Infiltration in Hepatocellular Carcinoma: Immune Cell Profiling Using the CIBERSORT. *Ann Transl Med* (2020) 8:1483. doi: 10.21037/atm-20-5830

37. Miao YR, Zhang Q, Lei Q, Luo M, Xie GY, Wang H, et al. ImmuCellAI: A Unique Method for Comprehensive T-Cell Subsets Abundance Prediction and Its Application in Cancer Immunotherapy. *Adv Sci (Weinh)* (2020) 7:1902880. doi: 10.1002/advs.201902880

38. Li T, Fu J, Zeng Z, Cohen D, Li J, Chen Q, et al. TIMER2.0 for Analysis of Tumor-Infiltrating Immune Cells. *Nucleic Acids Res* (2020) 48:W509–509W514. doi: 10.1093/nar/gkaa407

39. Chen Y, Li ZY, Zhou GQ, Sun Y. An Immune-Related Gene Prognostic Index for Head and Neck Squamous Cell Carcinoma. *Clin Cancer Res* (2021) 27:330–41. doi: 10.1158/1078-0432.CCR-20-2166

40. Reading JL, Gálvez-Cancino F, Swanton C, Lladser A, Peggs KS, Quezada SA. The Function and Dysfunction of Memory CD8+ T Cells in Tumor Immunity. *Immunol Rev* (2018) 283:194–212. doi: 10.1111/imr.12657

41. Kaseb AO, Vence L, Blando J, Yadav SS, Ikoma N, Pestana RC, et al. Immunologic Correlates of Pathologic Complete Response to Preoperative Immunotherapy in Hepatocellular Carcinoma. *Cancer Immunol Res* (2019) 7:1390–5. doi: 10.1158/2326-6066.CIR-18-0605

42. Wan S, Zhao E, Kryczek I, Vatan L, Sadovskaya A, Ludema G, et al. Tumor-Associated Macrophages Produce Interleukin 6 and Signal *via* STAT3 to Promote Expansion of Human Hepatocellular Carcinoma Stem Cells. *Gastroenterology* (2014) 147:1393–404. doi: 10.1053/j.gastro.2014.08.039

43. Facciabene A, Peng X, Hagemann IS, Balint K, Barchetti A, Wang LP, et al. Tumour Hypoxia Promotes Tolerance and Angiogenesis *via* CCL28 and T (reg) Cells. *Nature* (2011) 475:226–30. doi: 10.1038/nature10169

44. Wen ZF, Liu H, Gao R, Zhou M, Ma J, Zhang Y, et al. Tumor Cell-Released Autophagosomes (TRAPs) Promote Immunosuppression Through Induction of M2-Like Macrophages With Increased Expression of PD-L1. *J Immunother Cancer* (2018) 6:151. doi: 10.1186/s40425-018-0452-5

45. Sun C, Sun HY, Xiao WH, Zhang C, Tian ZG. Natural Killer Cell Dysfunction in Hepatocellular Carcinoma and NK Cell-Based Immunotherapy. *Acta Pharmacol Sin* (2015) 36:1191–9. doi: 10.1038/aps.2015.41

46. Shen H, Wang Z, Ren S, Wang W, Duan L, Zhu D, et al. Prognostic Biomarker MITD1 and Its Correlation With Immune Infiltrates in Hepatocellular Carcinoma (HCC). *Int Immunopharmacol* (2020) 81:106222. doi: 10.1016/j.intimp.2020.106222

47. Charoentong P, Finotello F, Angelova M, Mayer C, Efremova M, Rieder D, et al. Pan-Cancer Immunogenomic Analyses Reveal Genotype-Immunophenotype Relationships and Predictors of Response to Checkpoint Blockade. *Cell Rep* (2017) 18:248–62. doi: 10.1016/j.celrep.2016.12.019

48. Giannini EG, Aglitti A, Borzio M, Gambato M, Guarino M, Iavarone M, et al. Overview of Immune Checkpoint Inhibitors Therapy for Hepatocellular Carcinoma, and The ITA.LI.CA Cohort Derived Estimate of Amenability Rate to Immune Checkpoint Inhibitors in Clinical Practice. *Cancers (Basel)* (2019) 11(11):1689. doi: 10.3390/cancers11111689